2022

Integration of a Cooling System Architecture with a Skin Heat Exchanger for High Thermal Loads in Fuel Cell Powered Aircraft

Saija Schaefer

Farid Quaium

Nick Muhsal

Arne Speerforck

Frank Thielecke

See next page for additional authors

Integration of a Cooling System Architecture with a Skin Heat Exchanger for High Thermal Loads in Fuel Cell Powered Aircraft

Saija SCHAEFER[1*], Farid QUAIUM[2], Nick MUHSAL[3], Arne SPEERFORCK[1], Frank THIELECKE[2], Christian BECKER[3]

[1] Hamburg University of Technology, Institute of Engineering Thermodynamics, Hamburg, Germany
+49 (0)40 42878-2596, saija.schaefer@tuhh.de
+49 (0)40 42878-3144, arne.speerforck@tuhh.de

[2] Hamburg University of Technology, Institute of Aircraft Systems Engineering, Hamburg, Germany
+49 (0)40 42878-8290, farid.quaium@tuhh.de
+49 (0)40 42878-8201, frank.thielecke@tuhh.de

[3] Hamburg University of Technology, Institute of Electrical Power and Energy Technology, Hamburg, Germany
+49 (0)49 42878-2382, nick.muhsal@tuhh.de
+49 (0)40 42878-3113, c.becker@tuhh.de

* Corresponding Author

ABSTRACT

In this study, the application of heat sinks for cooling heat loads in a commercial aircraft is investigated. An outer skin heat exchanger is modeled numerically and examined. For this purpose, a suitable CFD (computational fluid dynamics) model of the heat exchanger is developed and validated. A well-founded evaluation of different geometry variants of the heat exchanger liquid side is carried out using the generated model. Subsequently, the designed geometries are evaluated with regard to their weight properties, which are of vital importance in the application of commercial aircraft. The received information at component level in combination to a defined cooling system architecture is used as an input for a developed overall system design methodology. Within this framework, a multi-criteria evaluation of the overall system level will show the influence of parameter variation on a component level and its effect on the overall system level for a regional aircraft. In particular, the required power demand, the resulting system weight and the induced aerodynamic drag are considered. Subsequently, an integration analysis of the selected system architecture is performed and evaluated in terms of plausibility.

1. INTRODUCTION

Due to society's increasing demand for CO_2-neutral propulsion methods, the electrification of aircraft is increasingly becoming the focus of current research. The use of fuel cells as a source of energy could be a possible way to achieve this. Fuel cells can be used to convert energy stored in hydrogen into electrical energy through a chemical reaction. The converted electrical energy is then used for, among other things, propulsion purposes. Since hydrogen is carbon-free, the sole reaction product is water, which can be released into the environment without negative environmental impact. If the hydrogen is produced using renewable energies, the fuel cell offers a climate-neutral propulsion method. Air cooling systems are in many cases not sufficient for adequate cooling in this technology. Therefore, liquid cooling systems are becoming indispensable. In many cases, they are much heavier than air cooling, which is why the overall weight in particular is a decisive aspect in the construction and design of cooling systems in commercial aircraft. The iTherNet (intelligent thermal network) research project revolves around the cooling of electrical heat sources, in particular fuel cell based propulsion systems, through optimized thermal system architectures.

2. METHODOLOGY

In order to generate a meaningful simulation model, complex framework conditions must be abstracted and simplified. PEM (Polymer Electrolyte Membrane) fuel cells prove to be suitable for the usage in a commercial aircraft (Pratt et al.,). They require a coolant flow in the temperature range of 50 °C to 100 °C in order not to risk damage due to overheating. The inlet temperature of the coolant flow is assumed to be 80 °C. The outlet temperature should be 90 °C. The fuel cell system in this present work has a cooling load of 300 kW. Deionized water is used as the coolant due to its high specific heat capacity. The coolant circuit is examined in a single phase, so that no evaporation should occur under the assumed temperatures.

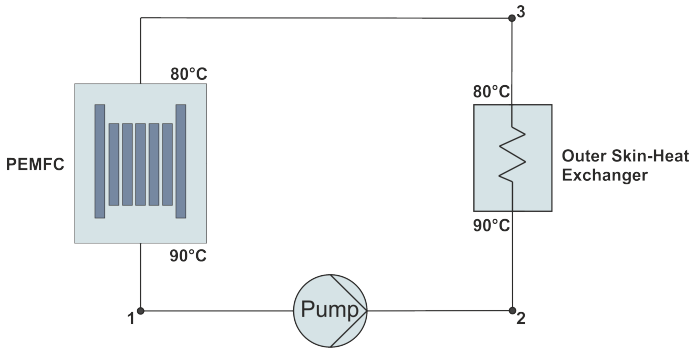

Figure 1: Scheme

The simplified circuit diagram for the coolant can be seen in figure 1. The pump is used to ensure flow of the coolant. The heat exchanger situated between state 2 and 3 represents the outer skin heat exchanger that is tasked with fluid cooling. The second heat exchanger from state 3 to 1 symbolizes the fuel cell. The heat sink of the outer skin will be considered in simplified form in stationary flight (cruise). A typical cruising altitude for commercial aircraft is h = 11km ≈ 36000ft. At this altitude, the outside temperature is approx. -30 °C to -60 °C. To be able to estimate the heat flow that can be permanently dissipated as realistically as possible, the highest outside temperature is selected for the simulations. The heat transfer coefficient in flight on the outer skin of the aircraft is based on previous flight tests that were made within the research project. The framework conditions described are listed in the following table. Material values for air and water at the given temperatures and pressures are taken from the VDI Heat Atlas (VDI e. V.,) and are integrated into the simulation as temperature dependent functions.

Table 1: Assumptions made for stationary flight

General conditions	**Variable**	**Value**	**Unit**
cooling load	$\dot{Q}$	300	[kW]
coolant inlet temperature	T_{in}	100	[°C]
coolant outlet temperature	T_{out}	90	[°C]
air temperature at flight altitude	T_{air}	−30	[°C]
heat transfer coefficient	α	100	[W/m^{2}K]
thermal conductivity of the outer skin	λ_{OS}	130	[W/mK]
layer thickness of the outer skin	t_{OS}	5	[mm]
thermal conductivity of the SHX material	λ_{SHX}	237	[W/mK]
layer thickness of the SHX	t_{SHX}	10	[mm]

The heat exchanger directs the cooling liquid through a pipe along the inside of the airplane surface. The fluid cools down due to the colder outer surface and is then led to the fuel cell at the required temperature. The pipe running along the inside is examined in various geometry options for pressure losses and heat transfer. For reasons of weight, the outer layer of commercial aircraft consists of light materials. A frequently used material for this is aluminum or an aluminum alloy. The outer skin is therefore designed as an aluminum layer with a thickness of t_{OS} = 5 mm and a thermal conductivity coefficient of $\lambda_{\text{OS}} = 130 \frac{\text{W}}{\text{mK}}$. The distance of the fluid to the contact surface between the heat exchanger

and the outer skin is kept constant at the smallest point between the different geometry variants, with $t_{SHX} = 10\,mm$. Due to the previously mentioned properties and its high thermal conductivity of $\lambda_{SHX} = 237\,\frac{W}{mK}$, aluminum is also chosen as the material for the heat exchanger. Table 1 shows the assumptions for the outer skin.

2.1 Geometry Variants

Three different geometry variants of the tube in the heat exchanger are tested and compared with regard to pressure loss and heat transfer. The first design is a tube with a circular cross-section area. The second design is a cuboid and the third design is a flat tube. In order to be able to relate the three designs to each other, the hydraulic diameter is used as a comparison value.

$$d_h = \frac{4 \cdot A}{U}. \tag{1}$$

The hydraulic diameter of different tube variants is used to compare the pressure losses of non-circular tubes with circular tubes. The three basic pipe cross-sections can be seen in the following figure 2.

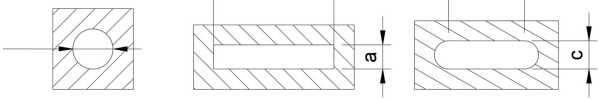

Figure 2: Geometry variants of the pipe cross sections

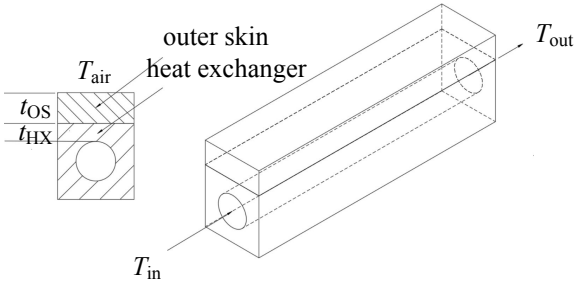

Figure 3: Heat exchanger

2.2 Building Model

The Siemens Star-CCM+ software is used for the numerical flow calculations. In addition to the geometry of the tube, the geometry of the heat exchanger block, in which the pipes are implemented, the surface of the aircraft and its surrounding air are also modeled. The mesh is a discretized representation of a geometric area for the calculation of discrete points. Siemens Star CCM+ solves the physical equations of the simulation only at the points defined by the mesh. Thus, the creation of the mesh has a major impact on the accuracy of the results (Ferziger,). For each of the modeled components, the mesh has to be adapted to the corresponding conditions. The tubes and the heat exchanger material are both modeled using a polyhedral mesh. These are particularly suitable for complex geometries and are also recommended for investigating heat transfer (Siemens Digital Industries Software,). The modeling of the boundary layer between the wall and the main flow has a decisive part in the accuracy of the results (VDI e. V.,). The flow boundary layer designates the area between the walls, in which the no-slip condition applies, and the outer flow, in which an approximately smooth behavior can be assumed (Ferziger,). There is a sharp increase in the velocity gradient in the flow boundary layer and a temperature transition between the outer flow and the wall temperature in the thermal boundary layer (Jiji,). In addition, the shear stress decreases with increasing distance from the wall. The change with increasing distance from the wall can be assumed to be negligibly small, which is why the wall shear stress is often used for modeling. Using the wall shear stress, another quantity can be introduced: the wall shear stress velocity u_τ, which is calculated using the following equation (Ferziger,):

$$u_\tau = \sqrt{\frac{\tau_W}{\rho}}. \tag{2}$$

The wall shear stress velocity u_τ describes the velocity close to the wall. Considering equation 2, a dimensionless wall distance can be defined as follows:

$$y^+ = \frac{u_\tau \cdot y}{\nu} \tag{3}$$

where ν represents the kinematic viscosity and y indicated the dimensional wall distance. The dimensionless coordinate y^+ is used to determine the area of the boundary layer in which the flow is located. Depending on the area either linear or logarithmic functions are then used for the flow calculation (Ferziger,). The Menter-Shear-Stress-Transport-Approach, also known as SST-k-ω-model, is used as the turbulence model in this study. This model combines the properties of

the most common turbulence models and offers the possibility to model the transition region with a sufficiently high level of accuracy (Siemens Digital Industries Software,). For more detailed definitions and equations for the SST-k-ω-model, please refer to the literature (Ferziger, ,).

As mentioned, modeling of the boundary layer is important for the accuracy of the results. In this study, a prism layer mesh is used for the coolant boundary layer and fitted to the geometry. Surface and air domain are meshed with trimmed cells. Here, the use of polyhedral meshes is dispensed in order to reduce the computational effort.

2.3 Verification

The outer skin heat exchanger, as used in this work, has not been extensively investigated so far. In order to verify the model nonetheless, the variables that occur, such as pressure loss and outlet temperature, are calculated using common relations from (VDI e. V.,) and compared with the simulated variables. Since the deviations are below 10%, the model is considered verified for further investigation.

Furthermore, a verification of the dimensionless wall distance y^+ is carried out. The comparison between the analytically calculated outlet temperature and the simulated outlet temperatures shows that the temperature error decreases for grids with a low y^+_{max}. Therefore, the dimensionless distance from the wall is reduced as far as possible, at least below $y^+_{max} = 5$, in order to confirm this assertion and to be able to minimize the error. The best result is achieved with the configuration that has the minimum dimensionless wall distance y^+_{max} of 1.2. There is only an error of 1.1% for the pressure calculation and 1.5% for the temperature calculation. Since the configuration used here has a value of low error, it is used for all further simulations.

3. CONCEPTUAL INTEGRATION AND EVALUATION STUDY

3.1 Overview of the Overall Aircraft System Design Framework GeneSys

The integration of new technologies, such as skin heat exchangers, requires systems architecture studies. For this reason, the Institute of Aircraft Systems Engineering (FST) at Hamburg University of Technology (TUHH) has developed the Overall System Design framework GeneSys(Jünemann et al.,). In general, the level of Overall Aircraft Design (OAD) represents the level of least detail, while the level of Detailed System Design represents the level of most detail during development. Both high, and low fidelity levels are connected via the Overall System Design (OSD) level. The implemented methodology enables parameterbased aircraft system design studies on OSD level. The Common Parametric Aircraft Configuration Schema (CPACS) is used as an interface to the OAD level. Based on the CPACS-interface, information such as aircraft geometry, performance and mission data are accessed, which represent the necessary high-level requirements of the OSD process. The required information from the preprocessing step can be used as an input for the subsequent generation of system topologies by means of component positioning and routing, after defining a logical and functional system architecture. By combining the information of the generated topology with theoretical equations, as well as empirical approaches, the system is underlying component can be sized and evaluated on the basis of chosen evaluation metrics (e.g. required power demand, system mass and system efficiency).

3.2 Aircraft and Cooling Architecture Definition

In the context of this paper, a concept plane that represents a typical size of a regional aircraft is chosen. The aircraft has ten propulsion nacelles (POD) and requires a maximum electrical power of approx. 3.65 MW. Each POD contains a fuel cell system, booster batteries and an electric drivetrain. It is assumed that the batteries do not require direct cooling during cruise conditions. Thus, a cooling concept with integration of skin heat exchangers can be implemented according to figure 5. The components to be cooled are focused on the electric drivetrain, consisting of electrical motor and power electronics, and fuel cells. It is necessary that the maximum operating temperature of the fuel cells (90 °C) and of the electrical components (75 °C) must not be exceeded.(Vredenborg,) Furthermore, it is assumed that the coolant is heated by the fuel cell system by a maximum of 10 °C and that the water contained in the exhaust gases exists in gaseous state.(Vredenborg,) The entire cooling circuit consists of the electric drive unit, the fuel cells, a pump for circulating the cooling medium and a coolant storage, which is used to counter system dynamics and prevent leakage losses. In addition, a parallel circuit consisting of the two heat sinks ram air-cooling and skin heat exchanger is integrated. In the scope of the evaluation, a comparative concept based on the same cooling circuit without skin heat exchanger is defined.

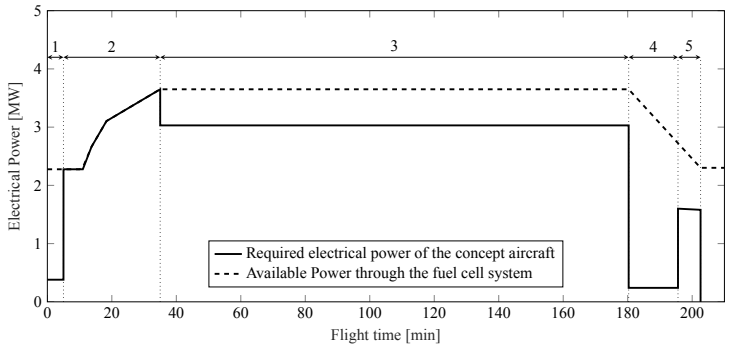

Figure 4: Power profile according to flight mission phases: 1=Taxiing, 2=Climb, 3=Cruise, 4=Descent, 5=Landing

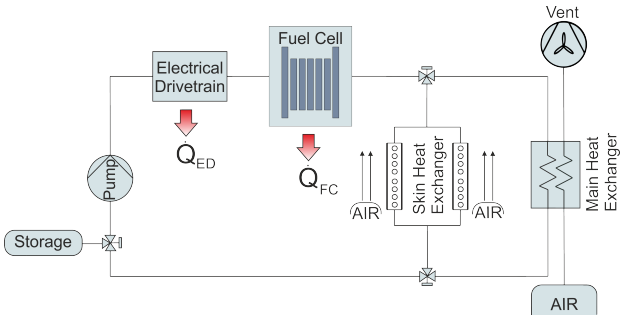

Figure 5: Defined cooling systems architecture with Skin Heat Exchanger within a POD of a conceptual aircraft

3.3 Preliminary System Sizing and Evaluation Approaches

To evaluate the two logical-functional system concepts, a simplified pre-dimensioning of components and cooling system is performed within the GeneSys framework. The inputs are the defined requirements and boundary conditions of flight envelope, aircraft, systems and the chosen components. The outputs are the resulting masses of the cooling system, the required electrical power demand, the resulting aerodynamic losses due to the high demand of air mass flow and the corresponding needs for large aircraft inlets, to transfer the generated thermal load to the environment. The calculations are based on thermal and material properties of the considered substances, the performance characteristics of the components, the determination of thermal loads of the propulsion components, as well as the fluid mechanical losses in the cooling circuit. The thermal loads of the propulsion components are determined by using the equations (4)-(6). To determine the heat load of the fuel cell, the operating characteristics of a commercial fuel cell with electrical power output of 125 kW is used. To avoid high thermal stresses on cell level, the design voltage is selected at the rated power of the fuel cell stack and not at the maximum power point of the fuel cell. This value can be obtained from the manufacturer's datasheets. In doing so, the electrical efficiency of the fuel cell is also expected to be higher. Depending on efficiency values, the heat load of the electric motor and converter can be determined. This facilitates to take technological improvements into account.

$$\dot{Q}_{\mathrm{FC,POD}} = P_{\mathrm{el.,POD}} \cdot \left(\frac{1.25}{U_{\mathrm{cell}}} - 1 \right) \tag{4}$$

$$\dot{Q}_{\mathrm{conv/motor}} = P_{\mathrm{el.,POD}} \cdot (1 - \eta_{\mathrm{conv/motor}}) \tag{5}$$

$$\dot{Q}_{\mathrm{ED}} = \dot{Q}_{\mathrm{conv}} + \dot{Q}_{\mathrm{motor}} \tag{6}$$

$$\dot{Q}_{\mathrm{tot.\ HL,\ POD}} = \dot{Q}_{\mathrm{FC,POD}} + \dot{Q}_{\mathrm{ED}} \tag{7}$$

Based on the resulting total heat load $\dot{Q}_{\mathrm{tot.HL,POD}}$, the main heat exchanger and the skin heat exchanger are dimensioned in dependency of the chosen cooling concept. A degree of hybridization between those heat sinks is determined according to (10). The cooling capacity of the skin heat exchanger is estimated according to the maximum available surface area of the fuel-less wing (approx. 40 m^2) and by taking component level characteristics according to (8) into account.

It is assumed, that the applied temperature difference and thermal resistance are constant. The cooling capacity of a skin heat exchanger unit per POD is determined by the use of (9).

$$\dot{Q}_{\mathrm{SHX,\,tot.}} = \frac{\dot{Q}_{\mathrm{SHX}}}{A_{\mathrm{ref.}}} \cdot A_{\mathrm{max.\ area,\ wing}} \tag{8}$$

$$\dot{Q}_{\mathrm{SHX,\,POD}} = \frac{\dot{Q}_{\mathrm{SHX,\,tot.}}}{N_{\mathrm{POD}}} \tag{9}$$

$$\gamma = \frac{\dot{Q}_{\mathrm{SHX,\,ref.}}}{\dot{Q}_{\mathrm{HX}}} \tag{10}$$

By applying the first law of thermodynamics under steady state conditions, and by using the specified degree of hybridization, given by (10) coupled with the given reference data at component level, the resulting mass of the skin heat exchangers per pod can be determined

$$m_{\mathrm{SHX,\,POD}} = m_{\mathrm{SHX,\,ref.}} \cdot \frac{\dot{m}_{\mathrm{cool,\,SHX}} \cdot c_{p,cool.}}{\dot{m}_{\mathrm{cool,\,ref.}} \cdot c_{p,\mathrm{cool.,\,ref.}}}. \tag{11}$$

Due to technological constraints, the entire thermal load generated by heat sources cannot be transferred to the environment by only using the skin heat exchanger. A main heat exchanger must be integrated into the system architecture. This heat exchangers design point is chosen in accordance with the top of climb point, which represents the end of the climb phase (figure 4). The determination of the mass of the main heat exchanger is not discussed in detail here. Approproate methods can be found e.g. in (Shah & Sekulić,). To determine the component properties (e.g. total mass, pressure losses, etc.) a level 2 approach is chosen by defining the internal geometries of the main heat exchanger. The physical states of the fluids are considered to be purely single-phase. To avoid high pressure losses, flat tubes are used on the coolant side. On the heat sink side, the ambient air serves as the cooling medium, which passes through a louvered fin geometry. The thermal design of the main heat exchanger is based on the ε-NTU method (Shah & Sekulić,). The required parameters can be taken from (Lüdders, Strummel, & Thielecke,). To determine the product of the thermal resistance and the surface of heat transfer, the heat transfer coefficient of the liquid side is determined using the Nusselt-Correlation described in (Vredenborg,). The heat transfer coefficient of the air side in the main heat exchanger is determined using a simplified stochastical approach for the Colburn factor by (Chang & Wang,). Subsequently, the total mass of the heat exchanger is calculated by adding the mass of the coolant to transport the maximum thermal load at the design point and the dry mass of the heat exchanger

$$m_{\mathrm{HX,\,POD}} = m_{\mathrm{HX,dry,\,POD}} + m_{\mathrm{cool,HX,\,POD}}. \tag{12}$$

The electrical power required to circulate the coolant is determined on the basis of the required volume flow, the pump efficiency, and the total pressure loss in the cooling circuit (15). The pressure loss of the fuel cells is determined by applying an experimental approach by (Vredenborg,). The pressure losses of the components of the electric drive train were calculated and subsequently validated by different manufacturer's data. The pressure losses on the coolant side of the main heat exchanger are modeled by employing the calculation method presented in (Churchill,). The pressure difference of a skin heat exchanger (SHX) unit per POD is calculated by the sum of the pressure differences of the reference element by multiplication with the ratio of the available SHX area per pod to the ref. area per SHX element (13). The mass of the pump can then be derived from a database given by the manufacturer's data, depending on the calculated power demand (16).

$$\Delta p_{\mathrm{SHX,\,POD}} = \Delta p_{\mathrm{SHX,\,ref}} \cdot \frac{A_{\mathrm{SHX,\,POD}}}{A_{\mathrm{SHX,\,ref.}}} \tag{13}$$

$$\Delta p_{\mathrm{tot,\,POD}} = \Delta p_{\mathrm{FC}} + \Delta p_{\mathrm{ED}} + \Delta p_{\mathrm{HX}} + \Delta p_{\mathrm{SHX}} + \Delta p_{\mathrm{pipe,\,tot}} + \Delta p_{\mathrm{ED}} \tag{14}$$

$$P_{\mathrm{Pump}} = \frac{\dot{V}_{\mathrm{cool,\,tot}}}{\eta_{\mathrm{Pump}}} \cdot \Delta p_{\mathrm{tot,\,POD}} \tag{15}$$

$$m_{\mathrm{Pump,\,POD}} = 0.0308 \cdot P_{\mathrm{Pump}} + 1.1912 \tag{16}$$

To counteract dynamic challenges of the rotating components and leakage losses at the cooling circuit, a coolant storage is integrated. The mass of the coolant storage is determined by estimating the storage geometry, the calculation norm

AD 2000 and using material properties e.g. of Al2219. To determine the minimum thickness of the storage (19), the resulting geometry is to estimate by determining the necessary fluid volume in storage (17) and the maximum pressure during the flight mission, the given material parameter and a safety factor. Due to atmospheric conditions defined at the International Standard Atmosphere by ICAO, the pressure decreases as the altitude increases. Hence, the for the design point of the storage the conditions on the ground are used. The total pressure to be considered is the sum of the atmospheric pressure at ground level and the hydrodynamic pressure due to the filling level (18). The necessary storage volume of the storage is calculated by the sum of the total fluid volume in pipes and the components. Since the fluid mass in the heat exchanger clearly predominates over the other components, it is used for the preliminary design studies. In addition, a dynamically induced volume loss due to the pump behavior is also calculated, so that the slip that occurs can be counteracted. By the assumption of a maximum storage diameter and storage volume of 30 % of the total volume of the cooling circuit, the storage height can be calculated.

$$V_{\text{tot, storage}} = 0.3 \cdot \left(V_{\text{tot, pipe}} + V_{\text{tot, comp.}} + V_{\text{dyn, Pump}}\right) \tag{17}$$

$$p_{\text{tot, storage}} = p_0 + \rho \cdot g \cdot h_{\text{fill}} \tag{18}$$

$$s_{\text{min.}} = \frac{p_{\text{tot, storage}} \cdot d_{\text{storage}}}{2 \cdot \frac{\sigma_{\text{Al2219}}}{S}} \tag{19}$$

$$m_{\text{storage, coolent, POD}} = V_{\text{shell}} \cdot \rho_{\text{Al2219}} \tag{20}$$

To determine the total mass of the cooling system, the sum of the total components mass and the total amount of fluid in the circuit is determined. The total mass of the components consists of the mass of the SHX, the mass of the main heat exchanger, the mass of the pump, the mass of the storage, the mass of the valves, and the mass of the mounting element of the pipes. The mass of each valves is assumed to be 1.5 kg. In the case of mounting elements, an increase of the piping mass by 15 % is calculated. The mass of the comparative architecture without SHX is reduced by the masses of the SHX, the associated coolant, piping, and mountings.

$$m_{\text{tot.}} = m_{\text{tot., comp.}} + m_{\text{tot., cool}} \tag{21}$$

In addition to determining the total mass (21) and the required electrical power demand (15), the air resistance induced as a result of the required cooling air mass flow is determined by the resolution of the impulse change of the air mass flow. In the course of the worst-case scenario, a complete deceleration of the air in the ram air duct is considered (22).

$$W_{\text{max.}} = \dot{m}_{\text{air,cruise}} \cdot \left(v_{\text{in}} - v_{\text{out}}\right) \tag{22}$$

To estimate the effect of the impact of the assessment metrics at aircraft level, the resulting fuel consumption of the individual elements is determined using the information in Table 2.

Table 2: Assumptions for the assessment of the evaluation metrics at aircraft level

Parameter	Variable	Value	Unit
Operating empty weight	m_{OEW}	17500	[kg]
Payload	m_{payload}	7100	[kg]
Fuel (LH2)	m_{fuel}	680.9	[kg]
Reserve fuel	-	0.1	[-]
Drag coefficient	c_{w}	0.5	[-]
Reference wing area	$S_{\text{W,ref}}$	66.1	[m]
Mach number	Ma	0.55	[-]

4. RESULTS

With the generated simulation model, results of the investigations regarding the pressure losses and heat transfer are shown in the following. The investigations are intended to show which of the various designed geometric variants is suitable for the application area of gas/liquid heat exchangers in commercial aircraft. In the next step, it is examined

over which pipe length the respective cross-section variants achieve cooling of the coolant from 363.15 K to 353.15 K. This length allows valid conclusions to be drawn about heat transfer and pressure losses in combination. The length required for cooling is decisive for the pressure losses and the weight. The pressure losses of the individual variants can be compared based on the pressure losses on the route up to the required cooling. For this, the pressure losses and the outlet temperature over the length of the pipeline are applied. In the next step, the temperatures are compared over the pipe length for the different cross-section variants. Figure 6 shows the coolant outlet temperatures over the pipe length for all seven geometry variants. The black line marks the coolant temperature of 353.15 K necessary for the fuel cell. The pipe length after which the outlet temperature of the fluid meets the requirement can be determined from the point of intersection of the temperature curves with the black line.

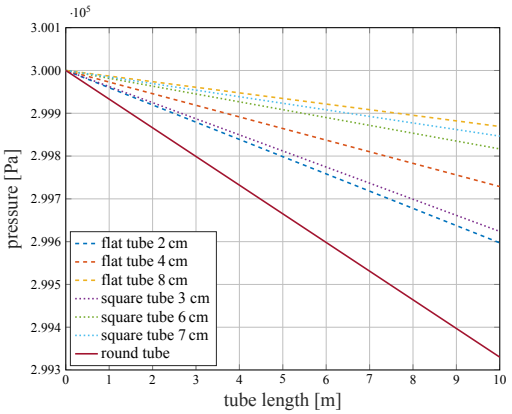

Figure 6: Coolant pressure over length

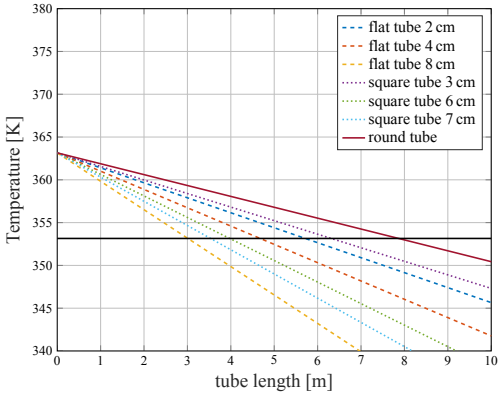

Figure 7: Coolant temperature over length

When looking at the table and the graph, it can be seen that the flat tube in the '8 cm' variant reaches the required temperature after the shortest length of tube through which flow has taken place. The temperature difference of 10 K is already reached after 3.01 m. The graph 6 shows that the pressure losses are also the lowest for the 8 cm flat tube geometry. This geometry variant is used for the following studies.

In the following, tests are to be carried out to determine which heat flows can be emitted through the outer skin. For this purpose, a heat exchanger consisting of a flat tube directs the refrigerant along the cold outer skin. The refrigerant flows into the heat exchanger at a temperature of 90°C and a mass flow of $\dot{m}_{\mathrm{HX}} = 0.233\,\mathrm{s}$. The pipes run in a U-shape with two consecutive 90° pipes with a distance of 0.05 m and a curvature radius of 0.075 m. The pipe length through which the gas flows is $l_{\mathrm{HX}} = 1.88\,\mathrm{m}$. The total area of the heat exchanger is therefore $A_{\mathrm{HX}} = 0.838\,\mathrm{m}^2$ and has a weight of 20.76 kg.

Figure 8 shows the temperature distribution of the flat tube in the middle of the heat exchanger and the surrounding material. The cooling of the coolant is shown with the color distribution in this figure 8. The main results of the CFD simulation study are:

- heat flux density $\dot{q}_{\mathrm{area}} = 5462.94\,\frac{\mathrm{W}}{\mathrm{m}^2}$
- heat flow per tube length $\dot{q}_{\mathrm{length}} = 2897.16\,\frac{\mathrm{W}}{\mathrm{m}}$

This stated results of the CFD study are subsequently incorporated into the Overall Aircraft System Design Framework GeneSys. By using the GeneSys framework, the thermal load along the flight mission is determined. The maximum total thermal load of approx. 350 kW occurs at the end of the climb phase. Figure 9 underlines that at the top of climb point, the largest share of the thermal load is produced by the fuel cells, being responsible for a thermal load of 329 kW. In cruise condition, the propulsion unit generates an amount of total thermal load of approx. 262.78 kW. Using the maximum integration ratio of the SHX, which is limited due to the available surface area of the wing, the SHX is only able to transfer heat power in the order of 50.28 kW. In the scope of the design process, the evaluation criteria total mass, the induced air resistance due to the required cooling air mass flow, and the electrical power requirement for circulating the coolant were determined for two system architectures. The system architectures with a skin heat exchanger and the use of ram air as a heat sink is referred to as concept 1 and the system concept without a skin

heat exchanger is referred to as concept 2. Based on the selected assumptions and boundary conditions, the cooling architecture of concept 1 provides a system mass of 1126 kg per POD, while the system mass of concept 2 accounts for 215 kg per POD. The electrical power demand of 0.4 kW for concept 1, is also higher than the electrical power demand of 0.35 kW for concept 2. The induced drag of 519 N for concept 1 is lower than the induced drag of 641 N by the use of concept 2, under the assumption that the air mass flow is fully decelerated. Evaluating the concepts on aircraft level by determining the additional fuel demand illustrates that the influence of mass clearly outweighs the influence of the other evaluation metrics. Due to the small effects of the pump's required power demand compared to the provided power of the drive train, the additional required mass flow is negligible in this context. The integration of concept 1 results in an overall additional hydrogen demand of approx. 32.67 kg, where the system mass accounts for 95 % of that additional demand and only about 5 % stems from additional induced drag. The integration of concept 2 requires an additional hydrogen demand of 7.81 kg, where the system mass is responsible for 76 % and the additional drag for 24 % of the additional hydrogen demand. This analysis tends to confirm the assumption that the integration of SHX reduces the induced drag. However, the significantly higher system mass has an overall negative effect. In addition, a plausibility check by means of a virtual integration of the cooling circuit's components suggests a lack of space based on the currently assumed aircraft geometry (see Figure 10).

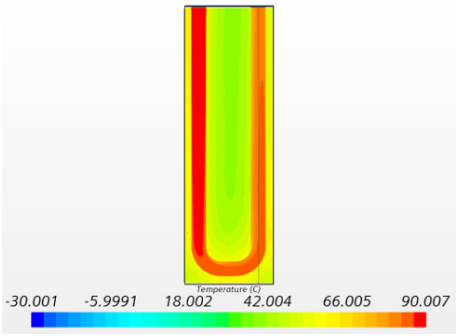

Figure 8: Temperature distribution of the outer skin heat exchanger

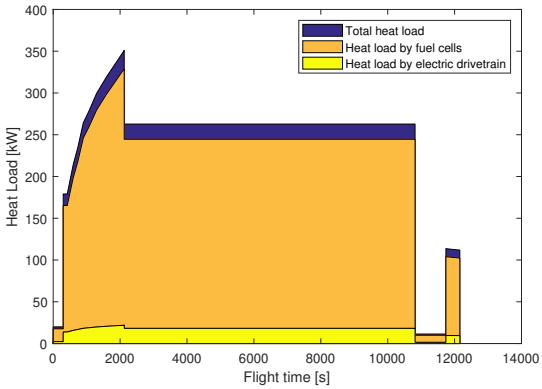

Figure 9: Total and component heat loads of propulsion unit

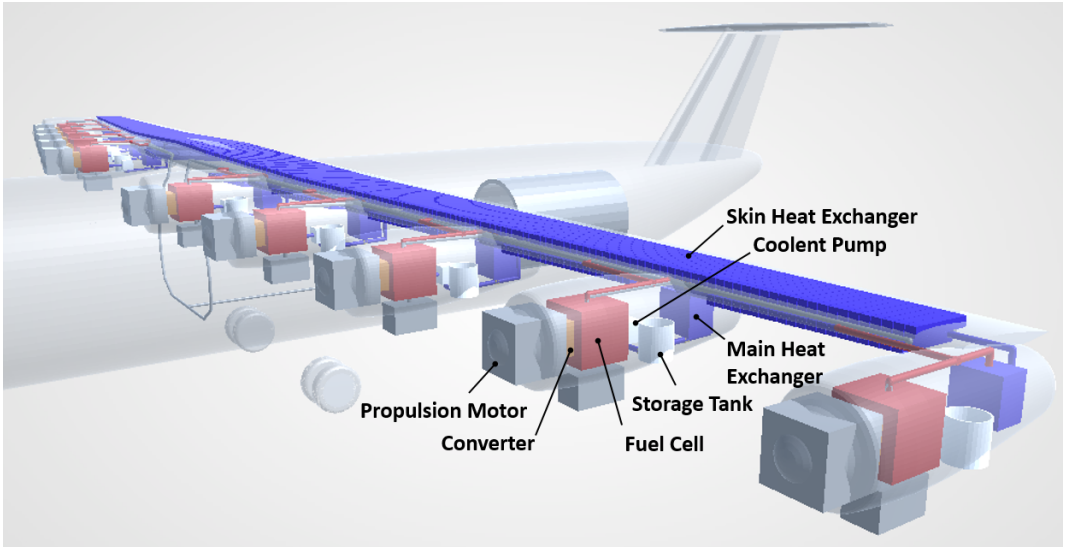

Figure 10: Illustration of the cooling architecture with Skin Heat Exchanger

5. CONCLUSION

In this paper, the integration of new cooling technologies for aircraft propulsion cooling is considered. The technologies are evaluated from the component to the aircraft level. The component level analysis shows that the highest performance characteristics can be obtained, when using flat tubes as internal geometries of the SHX. The evaluation on system level has demonstrated that due to the high thermal load of the propulsion system, low specific cooling performance of SHX, and a small installation space, an integration of SHX in the fuel-less wing is not feasible. While the induced drag and power demand is reduced, the evaluation on aircraft level indicates that the significantly higher system weight leads to a substantial increase in additional hydrogen demand.

NOMENCLATURE

			Subscript	
γ	hybridisation degree	(-)	cell	single fuel cell
d_h	hydraulic diameter	(m)	comp	component
g	gravitational constant	($m^3kg^{-1}s^{-2}$)	conv	converter
h	hight	(m)	cool	coolent
L	length	(m)	dyn	dynamic
$\dot{m}$	mass flow	(kg/s)	ED	electric drivetrain
m	mass	(kg)	el.	electric
P	power	(W)	FC	fuel cell
$\dot{Q}$	heat flow	(W/m^2)	HL	heat load
p	pressure	(Pa)	HX	heat exchanger
ρ	density	(kg/m^3)	in	inlet
τ	shear	(Pa)	OS	outer skin
U	voltage	(V)	out	outlet
u	velocity	(m/s)	POD	POD
V	volume	(m^3)	ref	reference
v	kinematic viscosity	(Pas)	SHX	skin heat exchanger
W	drag force	(W)	tot	total
y^+	dimensionless wall distance	(-)	w	wall

REFERENCES

Chang, Y.-J., Wang, C.-C. (1997). A generalized heat transfer correlation for Iouver fin geometry. *International Journal of Heat and Mass Transfer*, *40*(3), 533–544. doi: 10.1016/0017-9310(96)00116-0

Churchill, S. (1977). Friction Factor Equation Spans All Fluid Flow Regimes. *Chemical Engineering*(7), 91-92.

Ferziger, J. H. (2020). *Computational methods for fluid dynamics* (4th ed. 2020 ed.; R. L. Perić Milovan; Street, Ed.). Cham: Springer. Retrieved from `https://doi.org/10.1007/978-3-319-99693-6`

Jiji, L. M. (2006). *Heat convection*. Springer-Verlag Berlin Heidelberg. Retrieved from `http://www.gbv.de/dms/hebis-darmstadt/toc/178435864.pdf`

Jünemann, M., Thielecke, F., Peter, F., Hornung, M., Schültke, F., Stumpf, E. (2019). Methodology for Design and Evaluation of More Electric Aircraft Systems Architectures within the AVACON Project. *Deutsche Gesellschaft für Luft- und Raumfahrt - Lilienthal-Oberth e.V.*. doi: 10.25967/480197

Lüdders, H. P., Strummel, H., Thielecke, F. (2013). Model-based development of multifunctional fuel cell systems for More-Electric-Aircraft. *CEAS Aeronautical Journal*, *4*(2), 151–174. doi: 10.1007/s13272-013-0062-3

Pratt, J. W., Klebanoff, L. E., Munoz-Ramos, K., Akhil, A. A., Curgus, D. B., Schenkman, B. L. (2013). Proton exchange membrane fuel cells for electrical power generation on-board commercial airplanes. *Applied Energy*. doi: 10.1016/j.apenergy.2012.08.003

Shah, R. K., Sekulić, D. P. (2003). *Fundamentals of heat exchanger design*. Hoboken NJ: John Wiley & Sons.

Siemens Digital Industries Software. (2020). Simcenter star-ccm+ 2020.1 | user guide [Computer software manual]. Retrieved 2020-12-07, from `www.siemens.com/mdx`

VDI e. V. (Ed.). (2010). *VDI heat atlas*. Springer Berlin Heidelberg. doi: 10.1007/978-3-540-77877-6

Vredenborg, E. (2015). *Modellbasierter Entwurf von Kühlsystemen für Brennstoffzellen in Verkehrsflugzeugen* (Dissertation). Hamburg University of Technology.